Direct evidence of N aggregation and diffusion in Au^+ irradiated GaN

W. Jiang,[a] Y. Zhang, and W. J. Weber
Pacific Northwest National Laboratory, Richland, Washington 99352

J. Lian and R. C. Ewing
The University of Michigan, Ann Arbor, Michigan 48109

(Received 6 March 2006; accepted 20 May 2006; published online 10 July 2006)

A surface amorphized layer and a buried disordered structure were created in gallium nitride (GaN) irradiated using 1.0 MeV Au^+ ions to fluences of 25 and 70 Au^+/nm^2 at room temperature. Bubbles of N_2 gas within both the amorphized and disordered GaN are formed. A gradient profile with a lower N concentration in the amorphized region is observed, which provides direct evidence of N loss by diffusion in the Au^+ irradiated GaN. These results are important to understanding the amorphization processes in GaN and may have significant implications for the design and fabrication of GaN-based devices. © *2006 American Institute of Physics*.
[DOI: 10.1063/1.2219418]

Gallium nitride (GaN) is a semiconductor material with outstanding properties, including a wide band gap (3.5 eV) and a high breakdown field (3 MV/cm). Currently, it is one of the most important materials for application in advanced optoelectronic devices operating in the red, green, blue, and ultraviolet ranges.[1,2] The material also has a great potential for use in high-temperature, high-power, and high-frequency electronic devices, such as switches and rectifiers in power control and distribution systems.[1] Previous reports[3–6] have indicated that GaN is rather resistant to ion-beam-induced amorphization. Prior to full amorphization, an intermediate stage of disorder saturation is formed. This stage contains stable basal-plane dislocation loops, stacking faults, and local regions of highly disordered structures.[7,8] Recently, microstructural evolution in the amorphization processes of Au^+ irradiated GaN has been studied.[9] The present work extends our previous studies[9] to the interstitial behavior in Au^+ irradiated GaN.

The GaN single-crystal films used in this study were epitaxially grown on sapphire substrates. Both ion implantation and disorder measurements were performed using a 3.0 MV tandem accelerator. Irradiation of the specimens was performed using 1.0 MeV Au^+ ions at an angle of 60° relative to the surface normal. This condition readily allows for the analysis of disorder profiles using 2 MeV He^+ Rutherford backscattering spectroscopy (RBS) along the ⟨0001⟩-axial channeling direction (RBS/C). Ion fluences of 25 and 70 Au^+/nm^2 at fluxes of 5.0×10^{11} and 2.7×10^{12} Au^+/cm^2 s were applied, respectively, at room temperature. A cross-sectional thin foil of GaN irradiated at the lower fluence was prepared for examination by transmission electron microscopy (TEM) using standard tripod wedge polishing, followed by ion thinning to electron transparency. High-resolution TEM (HRTEM) analysis was conducted using a JEOL 2010F microscope with a point-to-point resolution of 0.25 nm. For GaN irradiated to 70 Au^+/nm^2, the depth profiles for the Ga and N atomic fractions in the near-surface region were determined using time-of-flight energy elastic recoil detection analysis (ToF-E ERDA) with 43 MeV I^{10+} ions.[10] The forward scattering recoils of the target atoms were collected at a scattering angle of 43° relative to the primary I^{10+} beam, which was incident at an angle of 67.5° relative to the (0001) surface normal.

The profile of the relative disorder on the Ga sublattice in the irradiated GaN is shown in Fig. 1 (top left) as a function of depth. The relative Ga disorder (fraction of the Ga displacements from their original lattice sites) is obtained from the He^+ ion-channeling spectra (not shown) using an iterative procedure.[11] The depth, which is derived from the ion backscattering energy, is referenced to the density of a perfect GaN crystal (6.1 g/cm^3). The RBS/C data suggest two distinctive stages in regions (a) and (b), corresponding to full amorphization and disorder saturation stages, respectively, which is consistent with previous reports.[3,6] This structure is also confirmed by the subsequent TEM observation shown in Fig. 1 (top right), where the amorphized and

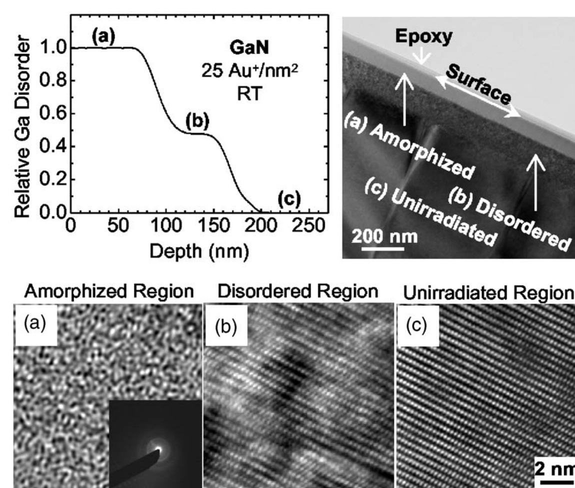

FIG. 1. Depth profile of the relative disorder on the Ga sublattice (perfect crystal=0; full amorphization=1) in GaN irradiated to 25 Au^+/nm^2 at room temperature (top left). The top-right TEM image shows a general view of the irradiated GaN that contains amorphized and disordered regions. The bottom three micrographs show high-resolution cross-sectional TEM images in different depth regions, corresponding to (a) the amorphized region, (b) the disordered region, and (c) the unirradiated region. The three images have the same magnification.

[a]Author to whom correspondence should be addressed; electronic mail: weilin.jiang@pnl.gov

 © 2006 American Institute of Physics

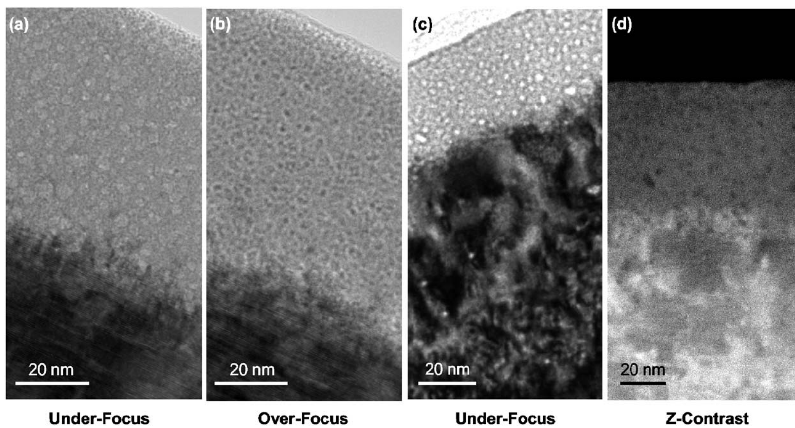

FIG. 2. Bright-field cross-sectional TEM images of N_2 bubbles/voids in the irradiated GaN (25 Au^+/nm^2) with (a) underfocus and (b) overfocus contrasts. (c) An underfocus bright-field image of bubbles/voids in a thinner region (the original surface was removed in the ion-thinning step). (d) A high-angle annual dark-field scanning TEM (STEM) image (*Z* contrast) of the irradiated GaN, showing a distribution of smaller bubbles/voids in the disordered region.

disordered layers are clearly resolved. The HRTEM images at a greater magnification in Figs. 1(a)–1(c), show the microstructures in the three depth regions. In contrast to the unirradiated region [Fig. 1(c)], the microstructure in the disorder saturation region [Fig. 1(b)] contains planar defects, which are similar to those that have been observed previously in ion-irradiated GaN.[7,8] The image in Fig. 1(a) was taken from the near-surface region where the crystal was fully amorphized. The inserted electron diffraction pattern in Fig. 1(a) shows diffuse diffraction rings that are characteristic of amorphous materials. This fully amorphized state is a result of further microstructural evolution of the locally amorphized zones and small randomly oriented crystalline domains, as discussed in the recent study.[9]

A more careful examination of the amorphized layer reveals a dense array of small bubble like structures, as shown in the bright-field images of Figs. 2(a) and 2(b). By changing the defocus values from underfocus to overfocus, the contrast of the microstructural feature changes from a white to darker color, thus confirming that these structures are bubble—or void-related features. Previous studies[12] of Au^+ irradiated GaN have indicated that a great majority of these structures are a result of N_2 bubble formation in the amorphized GaN. Some of the bubbles in this study could have been ruptured during the preparation of the cross-sectional TEM specimen, leaving behind voidlike structures; others, however, would still be buried beneath the surface and intact. The average size of the bubbles/voids is on the order of several nanometers. However, the formation of real voids in GaN during the ion irradiation cannot be ruled out completely.[13] These voids are not intended for distinction from the ruptured or gas-filled bubbles in this study. In another disordered region, where the specimen is thinner because the original surface was removed during the ion-milling process, the TEM result [Fig. 2(c)] clearly shows that in addition to the large bubbles present in the amorphized layer, some smaller ones (white spots) appear in the disordered region. The specimen was also examined using a high-angle annual dark-field TEM (*Z* contrast), and the results are shown in Fig. 2(d). Along with the large bubbles (black spots) in the amorphized layer, much smaller ones (1 nm or less in size) are observed in the disorder saturation region, which are invisible in the bright-field image of Fig. 2(c). The results in Fig. 2 provide direct evidence that N interstitials migrate during the ion irradiation and nucleate into the molecular form (N_2) in both the disordered and amorphized regions of the Au^+ irradiated GaN at room temperature. With an increase of dose, more and more N interstitials become available and bubbles grow to a larger size[12] through diffusion and coalescence processes. The tiny bubbles filled with the high-pressure N_2 gas induce large lattice strains in the crystal structure, which could contribute to the disruption of the crystalline structure during the amorphization processes.

As a further step, mass transport of the Ga and N in the Au^+ irradiated GaN has been studied by profiling the sublattices as a function of depth. To date, quantitative depth profiles for either N or Ga in ion-irradiated GaN have not been reported. Kucheyev *et al.*[14] have assumed N loss in Au^+ amorphized GaN based on the increase of Ga scattering yield in RBS spectra. Since conventional RBS cannot well resolve N from the Ga spectra for GaN, a confirmation is still needed. A previous study[15] of Auger electron spectroscopy (AES) has suggested N loss in the top atomic layers of GaN exposed to Ar^+ or H_2^+ plasma; however, neither the damage level in GaN nor the amount of the N lost was determined.[15] In order to quantitatively investigate the interstitial redistribution and loss in the Au^+ irradiated GaN, the ToF-E ERDA method has been employed in this study, which allows a simultaneous analysis of N and Ga sublattices in the ion-irradiated GaN. In contrast to secondary ion mass spectrometry (SIMS), ToF-E ERDA uses high-energy ion beams and does not involve noticeable ion sputtering that would otherwise rupture the embedded N_2 bubbles and result in N loss prior to measurement.

The two-dimensional data (time of flight versus recoil energy) from the ToF-E ERDA experiments are plotted in Fig. 3(a) after subtraction of the background counts. All the elements indicated in the figure are well resolved, including the two thick curves for Ga and N, as well as the small amount of H (impurity), C (contamination), O (oxidation), and Au (implanted species). The iodine signal originates from both multiple scattering (portion at lower energy channels) and direct scattering from Au. These data allow for extraction of energy spectra for individual recoils (data not shown). Based on the spectra, the elemental depth profiles are determined with the correction of detection efficiency for each element.[10] The results for the atomic fractions of Ga and N in the Au^+ irradiated GaN are depicted in Fig. 3(b) as a function of depth. Also included in the figure is a depth profile of the relative Ga disorder obtained from RBS/C measurements. Again, the linear depth scale in nanometers is referenced to the perfect crystal density.

From Fig. 3(b), the N concentration exhibits a gradual decrease toward the surface in the amorphized region (from surface to a depth of ~110 nm), and the lowest N concentration near the surface corresponds to ~42 at. %, as com-

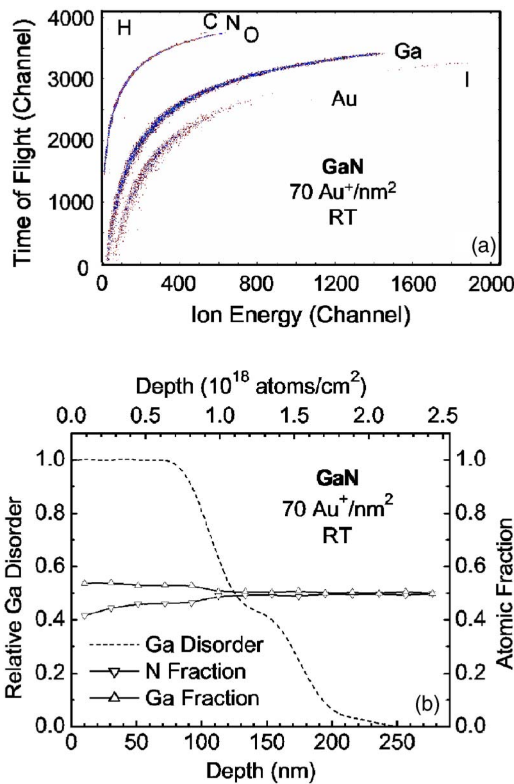

FIG. 3. (Color online) (a) ToF-E ERDA data plotted as the time of flight and energy of ions recoiled or scattered from GaN irradiated to 70 Au^+/nm^2 at room temperature. (b) Depth profiles of the Ga and N concentrations, determined using ToF-E ERDA. Also included is the relative Ga disorder as a function of depth, determined from RBS/C experiments.

pared to 50 at. % in the undamaged GaN (depth >250 nm). The results for an unirradiated area of GaN (data not shown) indicate a perfect stoichiometric balance of Ga and N of 50 at. % each in the surface region, as expected. The gradient in the N profile [Fig. 3(b)] suggests loss of N by diffusion and gas release during the Au^+ irradiation at room temperature. The N loss could also occur during the ERDA measurement (I^{10+} irradiation to ~0.1 ion/nm^2) at room temperature, but this contribution is insignificant as compared with that during the Au^+ irradiation (70 $ions/nm^2$) at similar temperatures. Supporting evidence from the ToF-E ERDA experiment includes no observable N loss either for an unirradiated specimen or for the Au^+ irradiated spot during sequential measurements. It is also interesting to note that a consistently lower N concentration (~49 at. %) appears in the disorder saturation region (110–180 nm). It is possible that similar to the N loss processes in the amorphized layer, the loss of N due to some diffusion in the disordered crystalline structure could be occurring, since N_2 bubbles are also formed in the same region [Figs. 2(c) and 2(d)]. Further studies are needed to fully understand the kinetics of N diffusion and bubble formation in the GaN crystal structure.

Again based on the data in Fig. 3(b), Ga atoms in the amorphized region are slightly enriched to ~53 at. % with a relatively flat depth profile. This enrichment is largely associated with the N depletion in the same depth region. The RBS result from this study confirms the Ga enrichment (data not shown), which is consistent with previous reports.[3,16] However, there is no evidence from this study that supports significant diffusion of Ga interstitials in the amorphized or disordered GaN at room temperature. This does not exclude the possibility of a short-range migration of Ga interstitials in GaN. In fact, previous experiments have suggested that Ga interstitials migrate in the crystal structure during ion irradiation even at low temperatures.[3,4,6,9] The migration and subsequent annihilation of point defects certainly enhance the efficiency of dynamic recovery during ion irradiation.[17] From Fig. 3(b), the atomic ratio of N to Ga in the amorphized GaN is between 0.77 at the surface and 0.87 near the interface of the amorphized and disordered layers under the experimental conditions.

In conclusion, N_2 gas bubbles are formed not only in the amorphized GaN but also in the disordered structures during Au^+ irradiation at room temperature. Nitrogen loss by diffusion occurs primarily in the amorphized GaN, leading to nitrogen depletion (42–46 at. %) and relative Ga enrichment (~53 at. %) in GaN irradiated to 70 Au^+/nm^2 at room temperature. It also appears that similar N diffusion and loss take place in the disordered GaN structure. No evidence has been found for significant Ga mass diffusion in the irradiated GaN at room temperature. The presence of the small N_2 bubbles in the crystal structure and the deficiency of the N concentration in the surface region may contribute to the reduced stability of the crystal structure, leading to full amorphization of GaN.

This research was supported by the Division of Materials Sciences and Engineering, Office of Basic Energy Sciences, U.S. Department of Energy. The experiments were completed in the Environmental Molecular Sciences Laboratory at the Pacific Northwest National Laboratory (Au^+ irradiation and RBS), in the Electron Microbeam Analysis Facility at the University of Michigan (TEM), and at the Uppsala University in Sweden (ToF-E ERDA).

[1] S. J. Pearton, J. C. Zolper, R. J. Shul, and F. Ren, J. Appl. Phys. **86**, 1 (1999).
[2] A. J. Steckl, J. C. Heikenfeld, D.-S. Lee, M. J. Garter, C. C. Baker, Y. Wang, and R. Jones, IEEE J. Sel. Top. Quantum Electron. **8**, 749 (2002).
[3] S. O. Kucheyev, J. S. Williams, and S. J. Pearton, Mater. Sci. Eng., R. **33**, 51 (2001).
[4] E. Wendler, A. Kamarou, E. Alves, K. Gärtner, and W. Wesch, Nucl. Instrum. Methods Phys. Res. B **206**, 1028 (2002).
[5] E. Alves, M. F. da Silva, J. C. Soares, R. Vianden, J. Bartels, and A. Kozanecki, Nucl. Instrum. Methods Phys. Res. B **147**, 383 (1999).
[6] W. Jiang, W. J. Weber, and S. Thevuthasan, J. Appl. Phys. **87**, 7671 (2000).
[7] C. M. Wang, W. Jiang, W. J. Weber, and L. E. Thomas, J. Mater. Res. **17**, 2945 (2002).
[8] Y. G. Wang, J. Zou, S. O. Kucheyev, J. S. Williams, C. Jagadish, and G. Li, Electrochem. Solid-State Lett. **6**, G34 (2003).
[9] W. Jiang, W. J. Weber, L. M. Wang, and K. Sun, Nucl. Instrum. Methods Phys. Res. B **218**, 427 (2004).
[10] Y. Zhang, H. J. Whitlow, T. Winzell, I. F. Bubb, T. Sajavaara, K. Arstila, and J. Keinonen, Nucl. Instrum. Methods Phys. Res. B **149**, 477 (1999).
[11] W. Jiang, W. J. Weber, C. M. Wang, L. M. Wang, and K. Sun, Defect Diffus. Forum **226-228**, 91 (2004).
[12] S. O. Kucheyev, J. S. Williams, J. Zou, and G. Li, Appl. Phys. Lett. **77**, 3577 (2000).
[13] T. Wójtowicz, F. Gloux, P. Ruterana, K. Lorenz, and E. Alves, Opt. Mater. (Amsterdam, Neth.) **28**, 738 (2006).
[14] S. O. Kucheyev, J. S. Williams, C. Jagadish, G. Li, and S. J. Pearton, Appl. Phys. Lett. **76**, 3899 (2000).
[15] X. A. Cao, S. J. Pearton, A. P. Zhang, G. T. Dang, F. Ren, R. J. Shul, L. Zhang, R. Hickman, and J. M. Van Hove, Appl. Phys. Lett. **75**, 2569 (1999).
[16] W. Jiang, W. J. Weber, S. Thevuthasan, and V. Shutthanandan, Nucl. Instrum. Methods Phys. Res. B **191**, 509 (2002).
[17] W. Jiang and W. J. Weber, Nucl. Instrum. Methods Phys. Res. B **242**, 431 (2006).